

FRAME SYNCHRONIZATION FOR PSAM IN AWGN AND RAYLEIGH FADING CHANNELS

Haozhang Jia

*Department of Electrical Engineering
University of Saskatchewan
Saskatoon, Canada, S7N 5A9
email: haj532@mail.usask.ca*

David E. Dodds

*Department of Electrical Engineering
University of Saskatchewan
Saskatoon, Canada, S7N 5A9
email: dodds@enr.usask.ca*

Abstract

Pilot Symbol Assisted Modulation (PSAM) is a promising method to compensate for fading in wireless land mobile communications. With PSAM, known pilot symbols are periodically inserted into the transmitted data symbol stream and the receiver uses these symbols to derive the amplitude and phase reference for data symbol detection

One aspect of this procedure that has not yet received much attention is frame synchronization, i.e. the technique used by the receiver to locate the time position of the pilot symbols in the received symbol sequence. This paper uses a non-coherent maximum likelihood (ML) frame synchronization approach in which only the magnitude of received signal is used to obtain the time position of the pilot symbols. Computer simulation results show good performance in both AWGN and fading channels and excellent tolerance to receiver frequency offset. Moreover, this method leads to simpler analysis and is somewhat simpler to implement.

Keywords: *Frame synchronization, PSAM, Maximum Likelihood Estimation.*

1. Introduction

One of the most devastating phenomena associated with mobile communications is channel fading, which can distort the transmitted signal severely and make the reception very difficult. It degrades the bit error rate and inhibits the use of spectrally efficient multilevel modulation schemes such as 16-QAM.

Pilot Symbol Assisted Modulation (PSAM) can reduce the impact of fading and facilitate the application of multilevel modulation schemes. PSAM has been studied by several researchers [1]-[4]. As illustrated in Fig. 1, known pilot symbols are periodically inserted into the data symbol stream and both data and pilot symbols are transmitted over communication channel. At the receiver, pilot symbols are separated from the data symbols and then used to derive the amplitude and phase reference for data symbol detection.

In our literature search, we find that one aspect of this process, frame synchronization, has been neglected in most research. Frame synchronization is the technique used by the receiver to identify the time position of the pilot symbol in received symbol sequence. We find the most applicable work in a paper by Gansman [5]. He presents two frame synchronization techniques: one is a maximum likelihood frame synchronizer and the other is a sequential testing algorithm. Both methods rely on coherent detection. This paper extends his work by applying a non-coherent approach to the maximum likelihood estimation algorithm. The new approach uses simplifying approximations based on relatively high SNR as consistent with the reception of 16-QAM. Computer simulation has been used to test synchronizer performance and several lengths and patterns of pilot symbol sequences were tested. Every 10th symbol was a pilot symbol and all other symbols were randomly selected data symbols.

This paper is organized as follows. The PSAM system and data model are presented in Section 2. Section 3 uses the maximum likelihood estimation formulation and develops a suboptimum frame synchronization technique based on high SNR approximations. Frame synchronization criteria for both AWGN and Rayleigh fading channel are introduced. Simulation results are presented and analyzed in Section 4, and concluding remarks follow as Section 5.

2. PSAM System Model

In the PSAM system model illustrated in Fig. 1, the transmitter periodically inserts specific pilot symbols into the data sequence. The combined pilot and data frame illustrated in Fig. 2 contains N pilot symbols inserted at intervals of L_p .

The composite symbol sequence $s(n)$ is linearly modulated by a square root raised cosine (Nyquist) pulse, $p(t)$ and then transmitted over a channel characterized by frequency non-selective slow fading and additive white Gaussian noise. Pilot symbols have the same pulse shape as the data symbols. The transmitted signal has a complex envelope given by,

$$s(t) = A \sum_{n=-\infty}^{\infty} s(n)p(t - nT_s) \quad (1)$$

where T_s is the symbol time, A is an amplitude factor, and $p(t)$, is a square root Nyquist pulse with unit energy such that:

$$R_p(t) = \int_{-\infty}^{\infty} p(\tau)p^*(\tau-t)d\tau \quad (2)$$

$$\text{and } R_p(kT_s) = \delta(k) \quad (3)$$

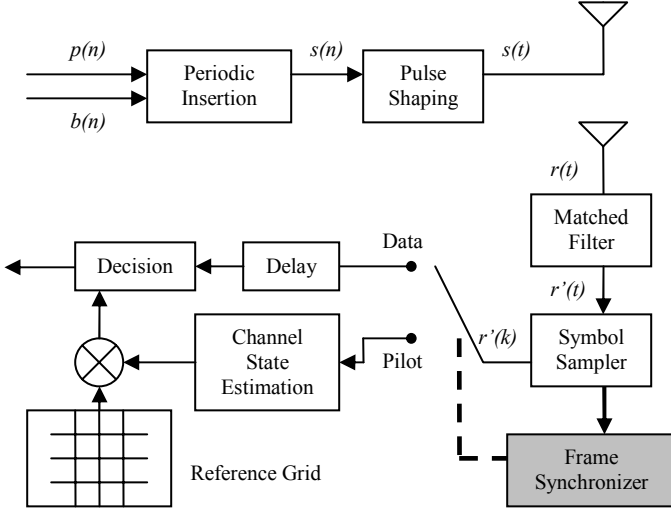


Fig. 1 PSAM system model

For frequency non-selective fading, the delay spread of the channel is much less than the symbol duration, i.e. all of the multi-paths arrive at receiver approximately at the same time. Therefore, the channel has no inherent intersymbol interference (ISI) and the multi-path distortion can be combined into one multiplicative distortion process $c(t)$. The received signal is then given by

$$r(t) = c(t)s(t) + n(t) \quad (4)$$

where $n(t)$ is zero mean AWGN with one-sided power spectral density N_0 . Passing this continuous received signal through a correlator matched to the pulse shape $p^*(-t)$ and sampled at the symbol times yields

$$r(kT_s) = A \sum_{n=-\infty}^{\infty} s(n) \int_{-\infty}^{\infty} c(\tau) p(\tau-nT_s) p^*(\tau-kT_s) d\tau + n(kT_s). \quad (5)$$

For slow fading, $c(t)$ is approximately constant over symbol duration T_s , so it may be pulled out of the integral as $c(k)$. Using (2) and (3), this is further simplified to

$$r(kT_s) = \sum_{n=-\infty}^{\infty} c(k)s(n)R_p((n-k)T_s) + n(kT_s) \quad (6)$$

and finally we obtain

$$r(k) = c(k)s(k) + n(k) \quad (7)$$

where $s(k)$ is a data symbol or pilot symbol, $n(k)$ is zero mean complex AWGN with variance N_0 , and $c(k)$ is the

multiplicative fading distortion factor, which has a Rayleigh magnitude distribution. The power spectrum of fading $c(k)$ is modeled as in [6],

$$E \{c_n c_{n-k}^*\} = \sigma_c^2 J_0(2\pi k f_D) \quad (8)$$

where J_0 is the zeroth-order Bessel function, σ_c^2 is the variance of the fading component, and f_D is the rms Doppler shift multiplied by the symbol time.

The idea behind PSAM system is clear. If the fading component $c(t)$ can be estimated accurately, then this channel state estimation can be used to counteract the fading effect and make the data decision more accurate. Frame synchronization is required in order to implement such a process [4]. As in Fig. 1, frame synchronization observes the received symbols and identifies the timing of the pilot symbols. Each pilot symbol gives a sample of channel state and these samples are then interpolated to form a continuous channel state estimation. This estimation is used to scale and rotate a reference decision grid and thus optimize the data output decision.

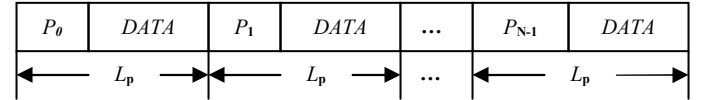


Fig. 2 PSAM frame format

3. ML Frame Synchronization Derivation

For a PSAM system, the frame synchronization must estimate the relative position of the first pilot symbol P_0 which corresponds to the start of a frame. Consider a full frame observation, \mathbf{x} , having length $L = L_p \times N$ with symbol index starting at 0,

$$\mathbf{x} = [x_0, x_1, x_2, \dots, x_n, \dots, x_{L-1}] \quad .$$

Let μ be the index of the pilot symbol P_0 within the full frame, where μ is an integer in the range $[0, L-1]$. The beginning of the frame (i.e., pilot symbol P_0) appears in any of the L positions in \mathbf{x} with equal probability. Therefore, maximum likelihood estimation is to search for the value of $\hat{\mu}$ that maximizes the function $f_x(\mathbf{x} | \mu)$ as given by

$$\hat{\mu}_{ML} = \underset{\mu \in [0, L-1]}{\operatorname{argmax}} f_x(\mathbf{x} | \mu) \quad (9)$$

where $f_x(\mathbf{x} | \mu)$ assesses the similarity between the known pilot sequence \mathbf{P} and the N received pilot-spaced symbols denoted \mathbf{x}^P starting at position $\hat{\mu}$ and expressed as

$$\mathbf{x}^P = \sum_{k=0}^{N-1} x_{kL_p + \hat{\mu}} \quad . \quad (10)$$

3.1. Synchronization in an AWGN Channel

The non-coherent frame synchronization scheme is based only on the magnitude of symbols and is thus insensitive to the phase and frequency offset in the receiver. In the square constellation of 16-QAM illustrated in Fig. 3, there are three levels of symbol amplitude. While any transmitted data symbol can take any one of the three levels, we restrict pilot symbols to the outermost circle or the innermost circle. Pilot symbols are therefore easily introduced into a sequence of 16-QAM data symbols.

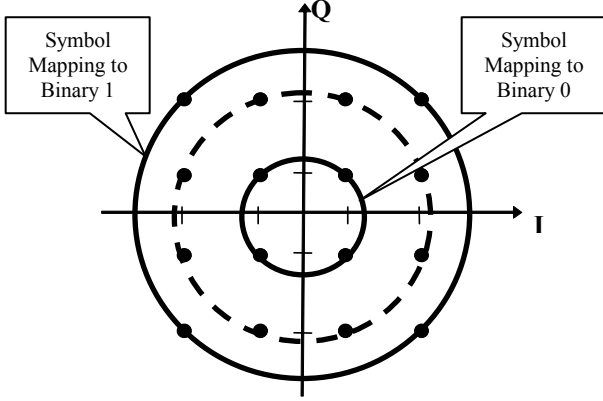


Fig. 3 Pilot Symbol mapping into 16-QAM

Let s denote the complex transmitted symbol, r denote the complex received symbol, and N_0 denote the power spectral density of complex AWGN having zero mean. It is well known [7] that, for an AWGN channel, the probability density function (PDF) of the received symbol is given as

$$f(r|s) = \frac{1}{\pi N_0} \exp\left(-\frac{|r-s|^2}{N_0}\right) \quad (11)$$

Because pilot sequence is presented here in magnitude, our interest is the probability density function of $|r|$ conditioned on $|s|$. Expressing complex symbols r and s in polar form and integrating equation over $\theta_r \in (0, 2\pi)$ yields

$$f(|r||s|) = \frac{|r|}{\pi N_0} \exp\left(-\frac{(|r|^2 + |s|^2)}{N_0}\right) \int_{2\pi} \exp\left(\frac{2|r||s|\cos(\theta_r)}{N_0}\right) d\theta_r \quad (12)$$

Using Bessel function of the first kind and zero order

$$I_0(x) = \frac{1}{2\pi} \int_{2\pi} \exp(x \cos \theta) d\theta \quad (13)$$

and substituting this Bessel function into the integral in (12), the probability density function becomes

$$f(|r||s|) = \frac{2|r|}{N_0} \exp\left(-\frac{(|r|^2 + |s|^2)}{N_0}\right) I_0\left(\frac{2|r||s|}{N_0}\right) \quad (14)$$

Changing the variables $|r|$ into $|r|^2$ and $|s|$ into $|s|^2$ yields

$$f(|r|^2 | |s|^2) = \frac{1}{N_0} \exp\left(-\frac{(|r|^2 + |s|^2)}{N_0}\right) I_0\left(\frac{2|r||s|}{N_0}\right) \quad (15)$$

Under high SNR, as it is in [8], the Bessel function can be approximated as

$$I_0(x) \approx \frac{\exp\left(|x| - \frac{1}{2} \ln|x|\right)}{\sqrt{2\pi}} \approx \frac{\exp(|x|)}{\sqrt{2\pi}} \quad (16)$$

Thus (15) is finally simplified as

$$f(|r|^2 | |s|^2) \approx \frac{1}{\sqrt{2\pi} N_0} \exp\left(\frac{(2|r||s| - |r|^2 - |s|^2)}{N_0}\right) \quad (17)$$

This conditional probability density function of magnitude squared received signal $|r|^2$ is similar to the Gaussian density distribution in terms of symbol magnitude $|r|$. However, this density function no longer integrates to 1 due to approximation factors. To maximize the likelihood function, as in [9], the following notations are defined:

\mathbf{P} --- pilot symbol sequence

$$\mathbf{P} = [|P_0|^2, |P_1|^2, \dots, |P_{N-1}|^2]$$

\mathbf{d}^p --- random data symbols spaced L_p symbol apart from each other when they appear in a full frame observation. The superscript \mathbf{p} stands for pilot spaced.

$$\mathbf{d}^p = [|d_0|^2, |d_1|^2, \dots, |d_{N-1}|^2]$$

\mathbf{r}^p --- the pilot-spaced observation, which is the collection of symbols within a full received frame starting at the 1st position and spaced apart from each other by L_p symbols.

$$\mathbf{r}^p = [|r_0|^2, |r_1|^2, \dots, |r_{N-1}|^2]$$

Note that elements in \mathbf{P} and \mathbf{d} must be the square of one of the three symbol magnitudes defined in the 16-QAM constellation (see Fig. 3). Both \mathbf{r}^p and \mathbf{d}^p are obtained by sampling the symbol stream at the pilot symbol spacing L_p . Therefore, by using (17), the frame synchronization problem of finding μ , the index of the pilot symbol P_0 within the full frame, becomes,

$$\hat{\mu}_{ML} = \underset{\mu \in [0, L-1]}{\operatorname{argmax}} \left(\frac{1}{\sqrt{2\pi} N_0} \prod_{i=0}^{N-1} \exp\left(-\frac{(|r_i| - |P_i|)^2}{N_0}\right) \right) \quad (18)$$

Where it is understood that pilot spaced sequence $r_0, r_1, r_2, \dots, r_{L-1}$ begins at the offset μ . The received symbol index $\mu + iL_p$ is modulo L and the pilot spaced symbols “wrap around” within the observed full frame. By taking the logarithm and neglecting terms that are unrelated to $|P|$, we obtain the maximum likelihood criterion for the AWGN channel,

$$\hat{\mu}_{ML} = \underset{\mu \in [0, L-1]}{\operatorname{argmax}} \left(\sum_{i=0}^{N-1} -(|r_i| - |P_i|)^2 \right) \quad (19a)$$

$$\hat{\mu}_{ML} = \underset{i}{\operatorname{argmax}} \left(\sum_{i=0}^{N-1} 2|r_i||P_i| - |r_i|^2 - |P_i|^2 \right) \quad (19b)$$

When viewed in N dimensional space, we select the received pilot spaced sequence that has the minimum Euclidean distance to the pilot sequence.

3.2. Synchronization in a Fading Channel

We now consider the frame synchronization problem in a Rayleigh fading channel. We assume a transmission model where all fading occurs at the transmitter; data symbols $|s(k)|$ are first modulated by fading signal $|c(k)|$, then the modified signal $|c(k)||s(k)|$ is transmitted over AWGN channel. This will give the same received signal as if data signal has been transmitted over a fading and noisy channel and is consistent with (7). Prior to synchronization, the magnitude of the channel fading signal can be reasonably estimated from pilot spaced observations of the received signal magnitude. In our analysis, we assume perfect estimation, which does not significantly degrade performance and greatly simplifies the computations. Following a similar procedure as we did for the AWGN channel, we scale the reference pilot sequence magnitude in (19) to yield the maximum likelihood criterion for Rayleigh fading channel

$$\hat{\mu}_{ML} = \underset{i}{\operatorname{argmax}} \left(\sum_{i=0}^{N-1} -(|r_i| - |c_i||P_i|)^2 \right) \quad (20)$$

In Section 4, Simulink® models are used to test the performance of both frame synchronizers with various pilot symbol sequences. The models implement the ML decision criteria above - an “*argmax*” structure indicates the most likely position of pilot symbol P_0 within a window length of L .

4. Simulation and Performance Analysis

In this study, data symbols and pilot symbols are both selected from 16-QAM data set. This differs from Gansman’s work [5] where data symbol are selected from the 16-QAM symbol set while pilot symbols are selected from the 8 PSK set. Pilot symbols are placed in the first position of every subframe, as illustrated in Fig. 2 and the pilot insertion interval is $L_p = 10$. The statistical performance of the synchronizer was tested with several pilot sequences that have good autocorrelation properties. These sequences were Barker code 7, 11, 13, Neuman-Hoffman 13 and PN 15 (see Table 1). For each case, one full frame observation is thus 70, 110, 130 and 150 symbols respectively. The simulation overview is illustrated in Fig. 4 and each data point used 100,000 trials of full frame observation.

The frame synchronizer output is compared to the output of a noise-free, error-free, simplified frame synchronizer and the number of correct synchronizations is recorded for 100,000 full frame observations. The signal generator continuously generates pseudo-random sequence and for each full frame observation, the frame synchronizer always generates an

estimate of pilot symbol P_0 . The transmitter of the simulation bench and the simplified transmitter of the reference bench work in a synchronized mode, so that they insert the same pilot symbol in exactly the same location of the symbol stream at the same time, estimates of pilot symbol P_0 , and never enter the verification mode. The result processor compares the output of the frame synchronizer to that of the simplified frame synchronizer, and counts the number of P_0 symbols that are correctly detected during 100,000 full frame observations.

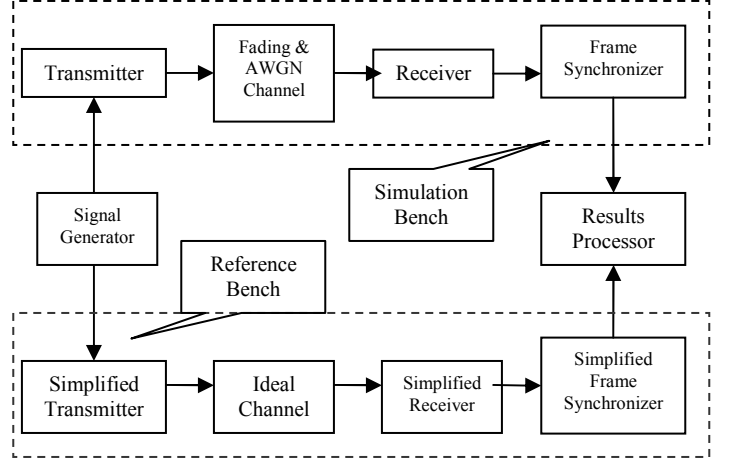


Fig. 4 Simulation test model

In computer simulation, AWGN is modeled by using the Simulink integrated block. SNR is defined by the ratio of the average power of input signal to noise power. Fading channel is modeled by a multi-path Rayleigh fading channel block Doppler fading rate was set to 1% of the symbol rate, which is consistent with that of [5].

Table 1

Sequence	Polar Binary Sequence
BK7	[-1,-1,-1,1,1,-1,1]
BK11	[-1,-1,-1,1,1,-1,1,1,-1,1]
BK13	[-1,-1,-1,-1,-1,1,1,-1,-1,1,-1,-1]
N-H13	[1, 1, 1, 1, 1, 1,-1, -1, 1, 1, -1, 1, -1]
PN15	[-1,1,1,1,-1,-1,-1,-1,1,-1,1,-1,-1,1,1]

Another characteristic of this frame synchronization method needs to be highlighted. Although it is usually assumed that carrier synchronization is achieved before frame synchronization, there is often some small frequency offset residue f_m . Moreover, fading channels introduce Doppler shift, f_D , which also causes frequency offset in the received signal. Thus it is instructive for us to test the frame synchronizer’s tolerance to these small frequency offsets. Therefore, the design parameter for an AWGN is SNR and frequency offset f_m , while the design parameters for Rayleigh fading channel are frequency offset f_m and Doppler shift f_D . The channel parameters f_m, f_D and SNR can significantly affect performance,

however, simulation shows our synchronizer to be robust to modest frequency offsets.

As in [5], our ML synchronizer is compared through simulation to the standard correlator and to the non-coherent synchronizer of Liu & Tan [8], which are, respectively,

$$\hat{\mu}_c = \underset{\mu \in [0, L-1]}{\operatorname{argmax}} \left| \sum_{k=0}^{N-1} p_k^* x_{kL_p + \mu} \right| \quad (21)$$

$$\hat{\mu}_l = \underset{\mu \in [0, L-1]}{\operatorname{argmax}} \left| \sum_{k=0}^{N-1} p_k^* x_{kL_p + \mu} \right| - f(x_{k+\mu}) \quad (22)$$

where $f(x_k)$ is a data correction term which we have chosen to be $|r|$ in our simulations. Fig. 5 compares simulated performance in AWGN and shows that our synchronizer performs much better than (21) and (22). In each case, BK11 was used as pilot sequence. Fig. 6 shows that on a fading channel with $f_D = 0.01$ of the symbol rate, our synchronizer performs well, while the others fail.

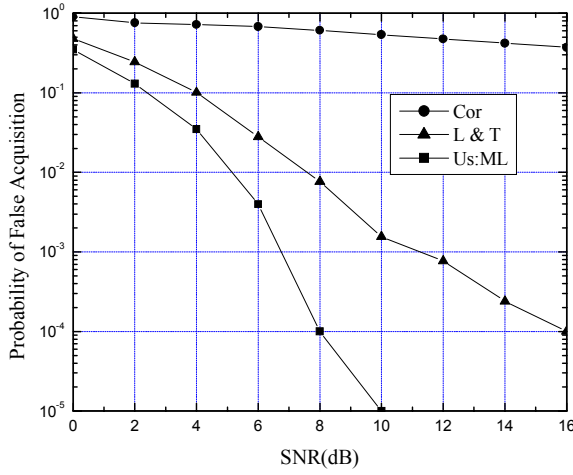


Fig. 5 Acquisition Performance in AWGN Channel with no receiver frequency offset and pilot sequence BK11

We now examine in more detail the probability of false acquisition as a function of pilot symbol bit pattern and channel SNR. Since SNR is generally not known, a range of values are explored. In addition, we calculate mean time to acquisition vs. SNR by the following expression of \bar{T}_{acq} that was adapted from [10]

$$\bar{T}_{acq} = T_f \left(\frac{1}{p_d^2} + \frac{1}{p_d} - \frac{1}{2} \right) + T_f p_f \left(1 + \frac{p_f}{(1-p_f)^2} \right) \left(\frac{1}{p_d^2} - \frac{1}{2} \right) \quad (23)$$

where $T_f = L = N * L_p$ is one frame period, p_d is the probability of true pilot symbol detection and p_f is the probability of false alarm, i.e. detection of a non-pilot symbol. Mean time to synchronization calculation was based on full frame ML observations and a verification stage that declares synchronization after two identical frame location estimates in succession.

The AWGN synchronizer has good performance over a wide range of SNR. Fig. 7(a) shows the probability of false acquisition of AWGN without frequency offset. The simulation results show that with the increase of the frame observation length, the probability of true pilot symbol detection increases, which is consistent with the theoretical analysis. To test the robustness of the synchronizer to frequency offset, we set frequency offset $f_m = 0.02$ as in [5]. The probability of false acquisition and the computed mean time to acquisition are shown in Fig. 7 (b) and Fig. 7(c) respectively. Simulation shows that although our frame synchronization method assumes high SNR, it also works well in moderate SNR.

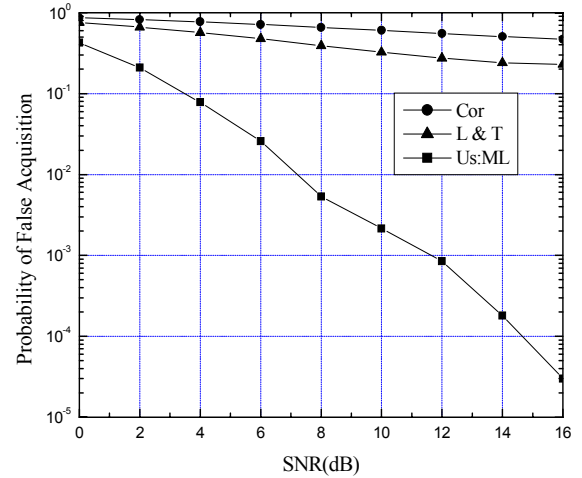


Fig. 6 Acquisition Performance in Fading Channel with $f_D = 1\%$ of the symbol rate and pilot sequence BK11

The performance in a Rayleigh fading channel is worse than for an AWGN channel. Fig. 8(a) shows the probability of false acquisition vs. SNR with parameters $f_D = 0.01$ and $f_m = 0.0$. The performance is especially poor at low SNR because of the high SNR approximation used in signal processing. Fig. 8(b) illustrates the probability of false acquisition vs. SNR for a Rayleigh fading channel with frequency offsets $f_D = 0.01$ and $f_m = 0.02$. Fig. 8(c) shows the mean time to acquisition for the same case with frequency offset. Frequency offset has little effect on the performance of the synchronizer and this is attributable to the non-coherent signal processing.

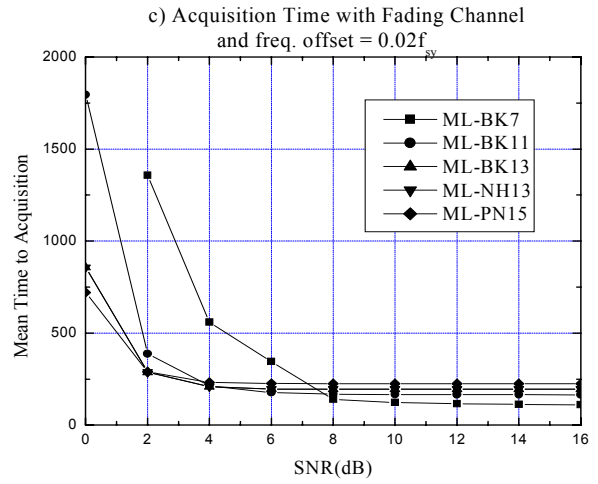
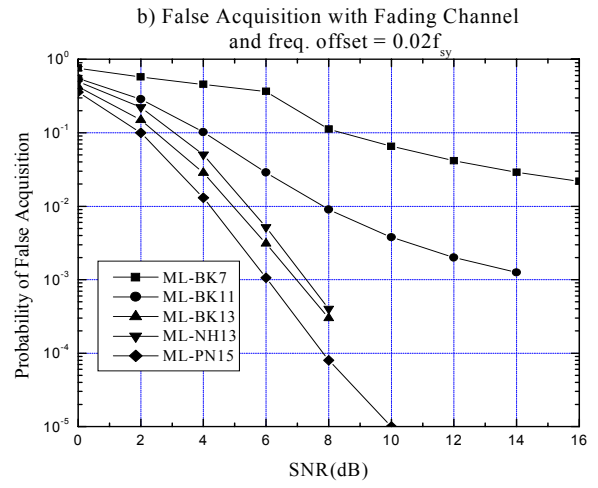
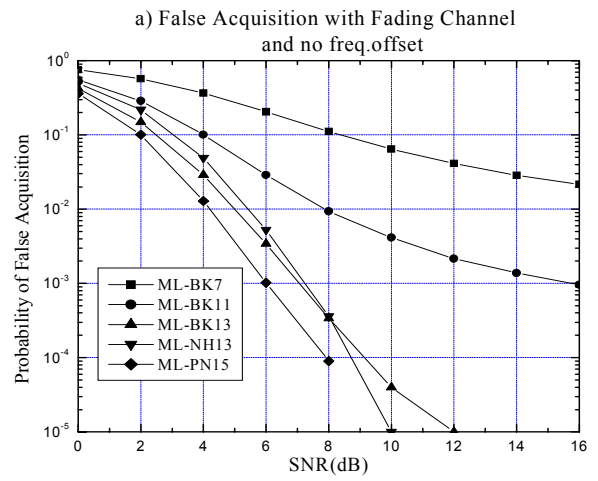
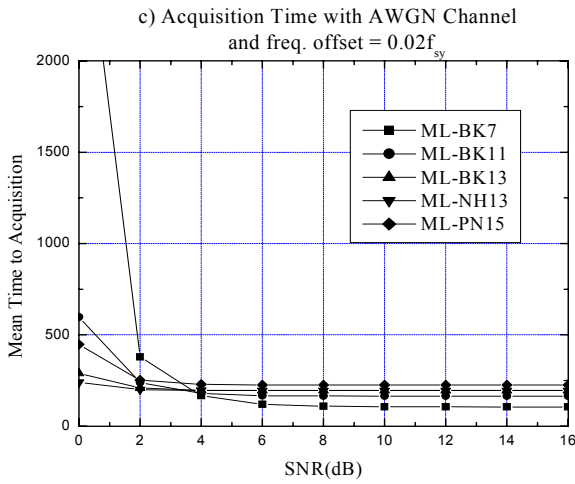
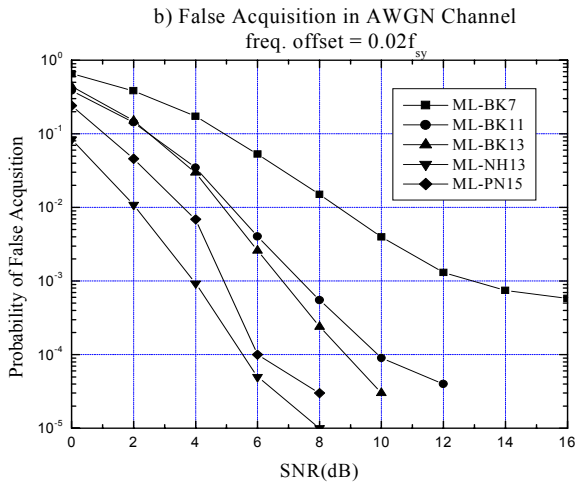
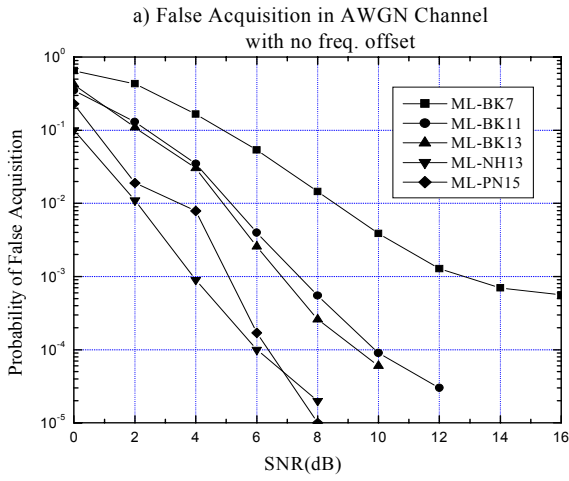


Fig. 7 Synchronization Performance in AWGN Channel
 a) with no receiver frequency offset,
 b) frequency offset = 2% of symbol rate and
 c) synchronization time with frequency offset

Fig. 8 Synchronization Performance in Fading Channel
 a) with no receiver frequency offset,
 b) frequency offset = 2% of symbol rate and
 c) synchronization time with frequency offset

5. Conclusion

In this paper, a non-coherent maximum likelihood frame synchronization technique for PSAM was developed and tested with AWGN and Rayleigh fading land mobile channels. When compared to a previous study using coherent detection [5], our non-coherent system shows somewhat better performance in both AWGN and fading channels and significantly better performance in presence of receiver frequency offset. In addition, our method leads to simpler analysis and is somewhat simpler to implement.

Acknowledgement

Student funding for this work was provided by a NSERC Discovery grant. Computing facilities were provided by the University of Saskatchewan and the authors are grateful for the assistance of Trevor Zintel and David Karaloff in setting up computing software.

References

- [1] J. H. Lodge and M. L. Moher, "TCMP-a modulation and coding strategy for Rician fading channels," *IEEE I. Select. Areas Commun.*, vol.7, pp 1347-1355, Dec.1989.
- [2] A. Aghamohammadi and H. Meyr, "A new method for phase synchronization and automatic gain control for linearly modulated signals in frequency flat fading," *IEEE Transactions on Communications*, vol. 38, pp.25-29, 1991.
- [3] J.K.Cavers, "An analysis of pilot symbol assisted modulation for rayleigh fading channels," *IEEE Transactions on Vehicular Technology*, vol.40, pp.686-693, November 1991.
- [4] S.Sampegi and T.Sunaga, "Rayleigh fading compensation for QAM in land mobile radio communications," *IEEE Transactions on Vehicular Technology*, vol.40, pp.137-147, May.1993.
- [5] A. Gansman, M.P. Fitz and J.V. Krogmeier, "Optimum and Suboptimum Frame Synchronization for Pilot-Symbol-Assisted-Modulation",*IEEE Transactions on Communications*, vol.45, No.10, pp.1327-1337, October 1997.
- [6] W. C. Jakes, "*Microwave Mobile Communications*," IEEE Press, 1974.
- [7] John G. Proakis, "*Communication systems engineering*," Prentice Hall, 1994.
- [8] G. L. Lui and H. H.Tan, Frame Synchronization for Gaussian Channels, *IEEE Trans. Commun.*, vol. COM-35, pp. 818-829, Aug. 1987.
- [9] D.E. Dodds, K. Takaya and Q. Zhang, "Frame Synchronization for Pilot Symbol Assisted Modulation"; Proceedings of IEEE Canadian Conference on Electrical and Computer Engineering, pp. 52-58, May 9-12, 1999, Edmonton, Canada.
- [10] B. Persson, D.E. Dodds, and R.J. Bolton, "A Segmented Matched Filter for CDMA Code Synchronization in Systems with Doppler Frequency Offset" Proceedings IEEE Globecom, San Antonio, Texas, Nov 2001.